Available online at www.sciencedirect.com
ScienceDirect
Journal of Molecular Catalysis A: Chemical 284 (2008) 16–23
JOURNAL OF MOLECULAR CATALYSIS A: CHEMICAL
www.elsevier.com/locate/molcata

Chemoselective synthesis of β-amino acid derivatives by hydroamination of activated olefins using AlSBA-15 catalyst prepared by post-synthetic treatment

Ganapati V. Shanbhag, S.M. Kumbar, S.B. Halligudi *

Inorganic Chemistry and Catalysis Division, National Chemical Laboratory, Dr. Homi Bhabha Road, Pune 411008, Maharashtra, India

Received 18 October 2007; received in revised form 20 December 2007; accepted 24 December 2007
Available online 4 January 2008

Abstract

β-Amino acid derivatives have a wide variety of applications *viz*. in the synthesis of peptide analogues, precursor for amino alcohols, optically active amino acids, lactums and diamines. Chemoselective anti-Markovnikov hydroamination reaction of activated olefins was effectively used to synthesize β-amino acid derivatives using AlSBA-15 and AlMCM-41 catalysts. These catalysts with different Si/Al ratios were synthesized by isomorphous substitution of aluminium into the framework of SBA-15, which induces the Brönsted and Lewis acid sites. The structural integrity of the catalysts was established by characterizing with XRD, N_2-sorption, TEM, NH_3-TPD, ^{27}Al MAS NMR and ^{29}Si MAS NMR techniques. Hydroamination of ethyl acrylate with aniline was used as a test reaction, which gave *N*-[2-(ethoxycarbonyl)ethyl]aniline with high selectivity. The performance of AlSBA-15 catalyst was also determined with different acrylates and amines to know the general applicability of the catalyst in hydroamination reactions.

Keywords: Mesoporous; Catalyst; AlSBA-15; AlMCM-41; Hydroamination; Addition; Acrylate; Amine; β-Amino acid; Activated olefin

1. Introduction

The catalytic addition of an N–H bond across a multiple bond (hydroamination), to give valuable nitrogen-containing molecules is of great interest to both academic and industrial researchers [1]. The hydroamination reaction proceeds with 100% atom economy which makes it one of the most desirable processes applicable in the area of natural products, pharmaceuticals, dyes, fine chemicals, polymers and surfactants [2]. A prime example for this type of reaction is the hydroamination of easily available olefins with amines. Regarding thermodynamics, the addition of amines to alkenes is approximately thermoneutral, whereas the corresponding addition to alkynes is slightly exothermic [3]. There are several reports on hydroamination of unactivated alkenes especially catalyzed by transition metal complexes in homogeneous and heterogeneous conditions [4–7]. On the other hand, hydroamination of activated olefins (acrylate derivatives) is a Michael type addition reaction, which is a simplistic approach to synthesize amino acid derivatives. These amino acid derivatives have a wide variety of applications *viz.* in the synthesis of peptide analogues, precursor for amino alcohols, optically active amino acids, lactums and diamines [8,9]. In earlier studies, Brönsted and Lewis acids such as H_2SO_4, HBF_4 and $FeCl_3$ have been used for this reaction [10,11]. Recently hydroamination of acrylates with amines has been reported with copper and bismuth salts [12,13], and complexes of Ni(II) and Pd(II) [14,15]. However, homogeneous methods suffer from tedious work-up procedures, low catalyst recyclability and above all the environmental problems. Scope of heterogeneous organic transformations is growing due to their well-documented advantages over homogeneous catalytic systems. But surprisingly there are very few reports available on the use of heterogeneous catalysts for hydroamination of activated olefins. Zeolite beta and clays have been reported so far for this reaction [16–19]. Zeolites cannot be used for larger substrates because of their smaller pore sizes, whereas clays have low thermal stability which affects the catalyst regeneration. Palladium complexes immobilized on silica and alumina surfaces have been reported for hydroamination of *O*-activated alkenes [20]. Mesoporous materials such as MCM-41 and SBA-15 have

* Corresponding author. Tel.: +91 20 25902107; fax: +91 20 25902633.
E-mail address: sb.halligudi@ncl.res.in (S.B. Halligudi).

1381-1169/$ – see front matter © 2008 Elsevier B.V. All rights reserved.
doi:10.1016/j.molcata.2007.12.025

advantages over zeolites for their larger pore size and higher surface area [21]. The isomorphous substitution of aluminium into the mesoporous framework of MCM-41 and SBA-15 induces the Brönsted and Lewis acidity [22]. AlSBA-15 has a larger pore diameter, thicker pore walls and higher hydrothermal stability compared to MCM-41. Hence AlSBA-15 has been used for hydroamination of activated olefins and the results are compared with that of AlMCM-41.

To create Brönsted and Lewis acidic sites in SBA-15, much effort has been made on the incorporation of heteroatom, such as Al, in the framework of mesoporous silica by post-grafting or doping (one-pot synthesis). However, it is very difficult to introduce the metals directly into SBA-15 due to the easy dissociation of metal–O–Si bonds under strong acidic conditions. Only a few studies on the direct synthesis of Al-SBA-15 have been reported so far [23–28]. Thus, the post-synthesis method for the alumination of mesoporous silicas, which are obtained by ion exchange, becomes a useful alternative. The researchers have demonstrated that Al can be effectively incorporated into siliceous MCM-41 and MCM-48 materials via various post-synthesis procedures [29–31]. The authors claimed that the materials produced via the post-synthesis method have structural integrity, acidity and catalytic activity similar to those of materials prepared by *in situ* method. However, as of present, very few post-synthesis alumination methods for SBA-15 have been reported [32–36]. In our earlier studies, we have successfully demonstrated montmorillonite clays and mesoporous materials as catalysts for intermolecular hydroamination of activated olefins and alkynes with amines [19,37–40]. The present study deals with the synthesis, characterization and the applications of AlSBA-15 in the synthesis of β-amino acid derivatives by the hydroamination of activated olefins with amines.

2. Experimental

2.1. Materials

Amines, solvents and metal acetates were purchased from Merck India Ltd. Activated olefins and montmorillonite K-10 were procured from Aldrich, USA. Zeolite H-beta was obtained from CPP, NCL, Pune. All the chemicals were of research grade and were used after drying following standard procedures.

2.2. Catalyst preparation

2.2.1. Synthesis of AlSBA-15

The synthesis of mesoporous silica SBA-15 was first reported by Stucky and coworkers [41]. In a typical synthesis, 4 g of amphiphilic triblock copolymer, poly(ethylene glycol)-block-poly(propylene glycol)-block-poly(ethylene glycol) (average molecular weight, 5800), was dispersed in 30 ml of water, and 120 g of 2 M HCl solution was added while stirring. 8 g of tetraethyl orthosilicate was then added to the homogeneous solution with stirring. This gel mixture was continuously stirred at 40 °C for 24 h and finally crystallized in a Teflon-lined autoclave at 100 °C for 2 days. After crystallization, the solid product was filtered, washed with distilled water, and dried in air at room temperature. The material was calcined in static air at 550 °C for 24 h to decompose the triblock copolymer and obtain a white powder SBA-15.

SBA-15 was used as the parent material to synthesize AlSBA-15 via a post-synthesis route similar to that reported elsewhere [32]. Series of AlSBA-15 catalysts (with Si/Al ratio ranging 10–40 taken in stoichiometric compositions during synthesis) were prepared using SBA-15. In a sample preparation, SBA-15 (1 g) was combined with 25 ml of dry ethanol containing different amounts of $AlCl_3$ with magnetic stirring at 80 °C for 10 h. The solid material was then filtered, washed vigorously with dry ethanol, and dried at room temperature in air to give AlSBA-15. It was calcined in static air at 550 °C for 5 h. AlMCM-41 was synthesized by following the procedure reported in our previous publication [42].

2.2.2. Synthesis of metal exchanged AlSBA-15

A known amount 1 g of AlSBA-15 (Si/Al = 10) was stirred with 0.05 M cupric acetate solution prepared in water (20 ml) at 80 °C for 6 h and then cooled to room temperature and the exchanged CuAlSBA-15 (10) was filtered, washed repeatedly with distilled water and dried in air. The above procedure was repeated to ensure maximum copper exchange. Then it was dried at 120 °C for 12 h and calcined (RT-500 °C, 4 °C min^{-1}; for 4 h at 500 °C). The similar procedure was followed for the preparation of ZnAlSBA-15 (10). These materials are designated as AlSBA-15-(X), MAlSBA-15 (X), where M is the exchanged metal ion and X is the Si/Al ratio of the chemical stoichiometric composition taken in the post-synthesis mixtures.

2.3. Characterization

Low-angle X-ray diffraction patterns of mesoporous samples were collected on a Philips X' Pert Pro 3040/60 diffractometer using Cu Kα radiation (l = 1.5418 Å), a nickel filter, and an X'celerator as a detector, using the real time multiple strip (RTMS) detection technique. XRD patterns were collected in the range of 2θ = 0.5–5.

The specific surface areas of the catalysts were measured by N_2 physisorption at liquid nitrogen temperature with an Omnisorb 100 CX (Coulter). Samples were dried at 300 °C in a dynamic vacuum for 2 h before the N_2 physisorption measurements. The specific surface area was determined using the standard BET method on the basis of adsorption data. The pore size distributions were calculated from both adsorption and desorption branches of the isotherms using the BJH method and the corrected Kelvin equation. Pore volume values were determined using the *t*-plot method of De Boer.

TEM photographs were obtained with a JEOL Model 1200 EX microscope operated at an accelerating voltage of 120 kV. Samples were prepared by placing droplets of a suspension of the sample in isopropanol on a polymer microgrid supported on a Cu grid for TEM measurements. SEM was used to characterize the surface morphology with a Leica stereoscan Cambridge 440 Microscope (UK) with a Kevex model EDAX system.

Magic angle spinning (MAS) NMR spectra for ^{27}Al and ^{29}Si nuclei were recorded on BRUKER DSX300 spectrome-

ter at 7.05 T (resonance frequencies 59.63 MHz, rotor speed 4000 Hz, number of scans 5275, external reference $Si(OCH_3)_4$ and 78.19 MHz, rotor speed 6000 Hz, number of scans 2800, external reference $Al(H_2O)_6^{3+}$ for ^{29}Si and ^{27}Al, respectively).

Acidity of the sample was measured by the TPD of adsorbed NH_3 (Micromeritics, Autochem 2910). The standard procedure for TPD measurements involved the activation of the sample in flowing He at 500 °C (3 h), cooling to 25 °C adsorbing NH_3 from a stream of He–NH_3 (10% NH_3 in helium), removing the physically adsorbed NH_3 by desorbing in He at 100 °C for 1 h and finally carrying out the TPD experiment by raising the temperature of the catalyst at 10 °C/min.

2.4. Catalytic activity measurements

Experiments were carried out in a two-necked round bottom flask fitted with a water condenser connected to a balloon filled with N_2 and kept in a thermostatic oil bath at a temperature of 100 °C at atmospheric pressure. In a typical reaction, ethyl acrylate (hereafter referred as EA) (1.04 g), aniline (0.96 g), toluene (3 ml) and catalyst (0.05 g, activated at 500 °C prior to reaction) were placed in the flask. The reaction was initiated by stirring the reaction mixture with a magnetic needle. Samples were withdrawn at regular intervals of time and analyzed by gas chromatography (Shimadzu 14B) equipped with a crosslinked 5% diphenyl–95% dimethylpolysiloxane capillary column (30 m) and a flame ionization detector. The identity of products were confirmed by GCMS (Shimadzu GCMS QP 5000) equipped with an identical column and a mass selective detector. Conversions were calculated with respect to weight percentage of EA. The product was separated by column chromatography using neutral alumina as stationary phase and petroleum ether/ethyl acetate, 95:5 as eluent. The single product was characterized by NMR, FTIR and GCMS analysis, which confirmed to be *N*-[2-(ethoxycarbonyl)ethyl]aniline. Yield: 95%, ^{1}HNMR (200 MHz, $CDCl_3$): 7.21–7.06 (*m*, 2H), 6.68–6.53 (*m*, 3H), 5.21 (1H), 4.13–4.01 (*m*, $J = 3.72$ Hz, 2H), 3.41–3.34 (t, $J = 6.45$ Hz, 2H), 2.57–2.47 (q, $J = 6.32$ Hz, 2H), 1.22–1.14 (t, $J = 7.07$Hz, 3H), FT-IR (neat) υ 3409, 2985, 1731, 1604, 1504, 1373, 1319, 1249, 1176, 1099, 1029, 1864, 748, 694. GCMS: *m/z* (relative intensity): 193 (11.83), 118 (2.55), 106 (100), 93 (2.46), 77 (11.26), 65 (6.57), 51 (7.79).

3. Results and discussion

3.1. Characterization of the catalysts

XRD patterns of calcined AlSBA-15 catalysts with different Si/Al ratios (shown in Fig. 1(a)–(d)) consist of three well-resolved peaks in the 2θ range of 0.8–1.8 correspond to the (1 0 0), (1 1 0) and (2 0 0) reflections which are associated with p6mm hexagonal symmetry in the materials. Isomorphous substitution of Al into the framework of siliceous SBA-15 by the post-synthesis method did not show any changes in the XRD pattern implying that the hexagonal mesoporous structure is retained after modification. It is evident from the XRD profile of the samples that they do not contain any other phase or amorphous matter. Also XRD pattern of AlMCM-41 (15) (Fig. 1(e)) shows (1 0 0), (1 1 0) and (2 0 0) reflections in lower 2θ region which demonstrates the well ordered nature of phases in the AlMCM-41.

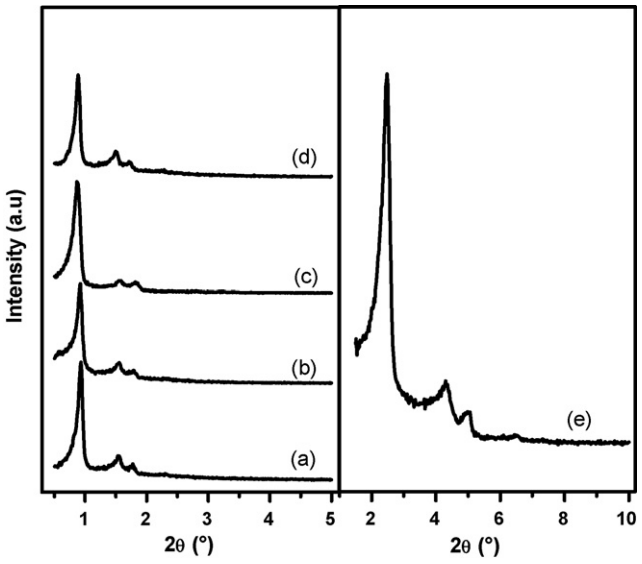

Fig. 1. Low angle XRD patterns of (a) AlSBA-15 (10), (b) AlSBA-15 (20), (c) AlSBA-15 (30), (d) AlSBA-15 (40) and (e) AlMCM-41.

Textural properties such as specific surface area, specific pore volume and mesopore size distribution are typically obtained from low-temperature (−196 °C) nitrogen adsorption isotherms. The nitrogen adsorption–desorption isotherms of AlSBA-15 (10) is shown in Fig. 2, and the textural properties of all the samples are presented in Table 1. All isotherms were of type IV, as defined by IUPAC and exhibited a H1-type broad hysteresis loop, which was typical of large-pore mesoporous solids. As the relative pressure increases ($p/p_0 > 0.6$), all isotherms exhibit a sharp step characteristic of capillary condensation of nitrogen within uniform mesopores, where the p/p_0 position of the inflection point is correlated to the diameter of the mesopore. The pore

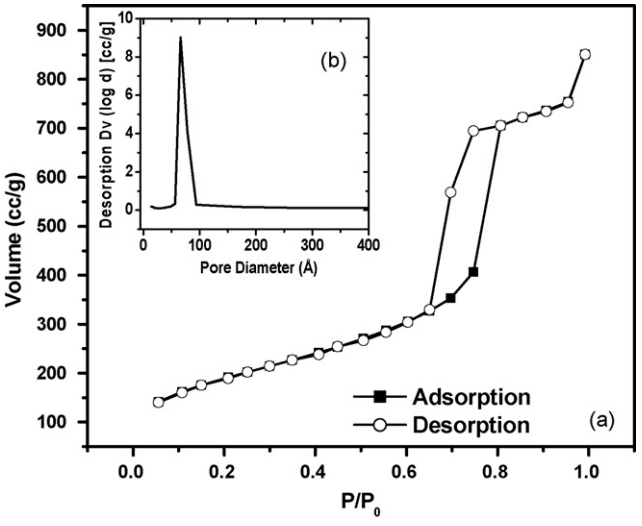

Fig. 2. N_2 adsorption and desorption isotherm (a) AlSBA-15 (10) and (b) inset picture: pore size distribution of AlSBA-15 (10).

Table 1
Structural characteristics and acidity of different catalysts and their catalytic activities

	Catalyst	Si/Al (XRF)	Surface area BET ($m2\ g^{-1}$)	Pore volume (cm3/g)	Average pore diameter (Å)	Total acidity (mmol NH_3/g)	EA conversion (wt.%)[a]	Mono-addition selectivity (%)	TOF[b]
1	SBA-15	∞	745	1.03	66.6	0.08	05	100	–
2	AlSBA-15 (10)	17	685	1.31	76.7	0.23	77	100	46
3	AlSBA-15 (20)	26	730	1.16	66.3	0.20	60	100	45
4	AlSBA-15 (30)	36	720	0.99	63.5	0.16	41	100	38
5	AlSBA-15 (40)	43	620	0.98	63.4	0.12	33	100	37
6	AlMCM-41 (15)	15	962	0.80	33.6	0.26	82	100	43
7	H-beta	15	530	0.28	–	–	41	99	18
8	Clay	–	230	–	–	–	39	99	–
9	CuAlSBA-15 (10)	20	664	1.09	67.9	–	50	100	32
10	ZnAlSBA-15 (10)	21	671	1.12	69.1	–	53	100	33

[a] Conditions: temperature = 100 °C, aniline to EA mole ratio = 1, catalyst wt. = 0.05 g, total reactants wt. = 2 g, toluene = 3 ml, time = 6 h.
[b] TOF = moles of EA converted per mole Al per hour.

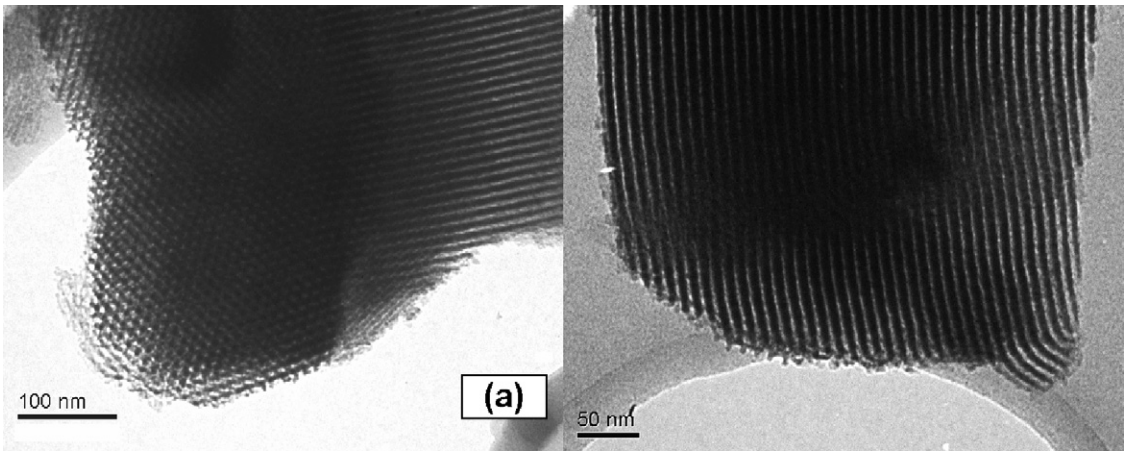

Fig. 3. TEM photographs of AlSBA-15 (10).

size distribution calculated from Kelvin equation is presented as a BJH plot (inset picture, Fig. 2). It showed a narrow pore size distribution with average mesopore size of 77 Å and a high surface area ABJH of 685 m^2/g. The overall N_2 adsorption amounts decreased depending on the aluminium loading though no particular trend was observed. Low alumination of SBA-15 did not affect the original pore structure of the parent SBA-15 while the surface areas slightly decreased with increase in aluminium loadings (Table 1). AlMCM-41 (15) had a higher surface area but lower average pore diameter than AlSBA-15 (10) (962 m^2/g vs. 685 m^2/g and 33.6 Å vs. 77 Å, respectively). Surface areas of H-beta (480 m^2/g) and montmorillonite K-10 (207 m^2/g) are low compared to AlSBA-15 catalysts.

TEM measurements were carried out to study the morphology of AlSBA-15 (10) (Fig. 3). TEM images of these catalysts show the retention of the periodic structure of parent SBA-15 precursor. It indicates that hexagonally arranged mesopores of SBA-15 are retained after modification with aluminium.

^{29}Si MAS NMR spectra (Fig. 4(i)) of SBA-15 (a) and AlSBA-15 (b) the samples contain a broad signal at −100 ppm and some shoulders at −90, −107 and −110 ppm. The main signal at −100 ppm is due to $Si(OSi)_3OH$ species (Q_3), while the shoulders at −90, −107 and −110 ppm are attributed to $Si(OSi)_2(OH)_2$ (Q_2), Si(3Si,1Al) and $Si(OSi)_4$ (Q_4) structural

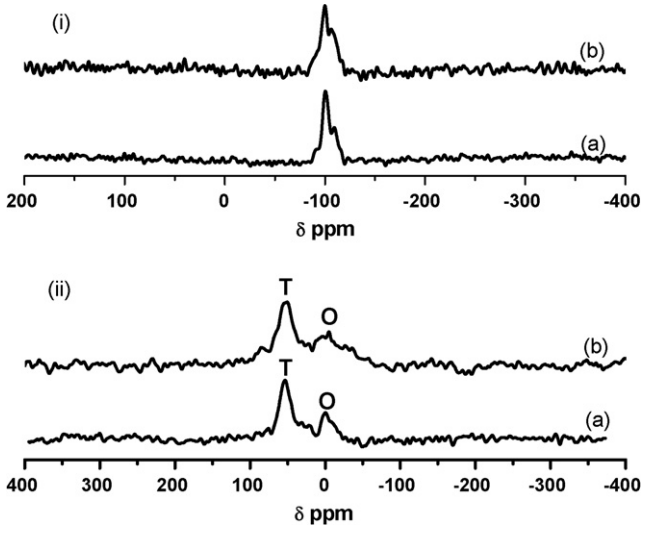

Fig. 4. (i) ^{29}Si MAS NMR profile of (a) SBA-15 and (b) AlSBA-15 (10). (ii) ^{27}Al MAS NMR profile of (a) AlSBA-15 (10) and (b) AlSBA-15 (30), (T = tetrahedral Al sites and O = octahedral Al sites).

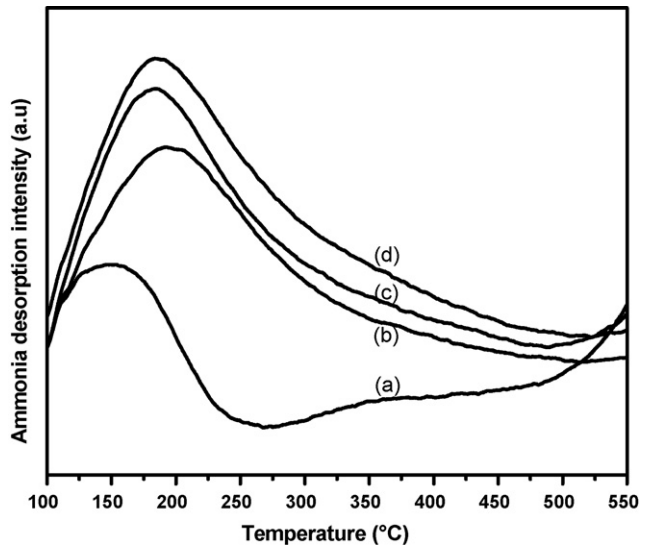

Fig. 5. NH_3-TPD profile of (a) SBA-15, (b) AlSBA-15 (30), (c) AlSBA-15 (20) and (d) AlSBA-15 (10).

units, respectively as reported Kolodziejski et al. [43]. There are no significant differences between ^{29}Si MAS NMR spectra of AlSBA-15 and SBA15. Moreover, the broadness of the 29Si signals has been attributed to the large distribution of the T–O–T angle.

Solid-state ^{27}Al MAS NMR was used to determine the local environment of aluminium in the AlSBA-15 samples. The spectra of AlSBA-15 (10) (Fig. 4(ii) (a)) and AlSBA-15 (30) (Fig. 4(ii) (b)) samples show that the majority of Al atoms are incorporated into the framework of SBA-15 (tetrahedrally coordinated, 53 ppm) in which Al is covalently bound to four Si atoms via oxygen bridges. The peak at 0 ppm is attributed to distorted or octahedrally coordinated aluminium species in extra-framework positions. In addition, low intensity signals were observed around 30 ppm which indicated the presence of distorted tetrahedral or five coordinated aluminium in SBA-15 [44].

The acidities of the AlSBA-15 and SBA-15 samples were measured by NH_3-TPD method and TPD profiles are depicted in Fig. 5. The total acidity data of SBA-15 and AlSBA-15 with different Si/Al expressed in mmol/g of desorbed ammonia are listed in Table 1. TPD plots of SBA-15 and AlSBA-15 show that there is a substantial increase in acidity and acid strength after aluminium incorporation in SBA-15. There is only one asymmetric broad peak on the TPD profiles of the AlSBA-15 samples. Total acidity increased with decrease in Si/Al ratio. This is due to the increase in number of acid sites on AlSBA-15 with a decrease in Si/Al ratio. Highest acidity was found to be 0.23 mmol of NH_3/g for AlSBA-15 with high Al content (Si/Al = 17). It is to be noted that pure mesoporous silica is acidic in nature though the acidity is low compared to AlSBA-15. SBA-15 showed total acidity of 0.08 mmol of NH_3/g. These results clearly indicated that the acid sites were formed after the alumination on the surface of the solid.

3.2. Catalytic results

Intermolecular hydroamination of EA with aniline to give *N*-[2-(ethoxycarbonyl) ethyl]aniline (Scheme 1) as the mono-addition product was chosen as a model reaction to test the performance of AlSBA-15 catalyst and comparing its activity with other catalysts montmorillonite K-10, H-beta and AlMCM-41. This reaction is highly selective and anti-Markovnikov mono-addition product was formed in a major amount under the reaction conditions studied. Since the mono-addition product contains N–H bond, it reacts further with another molecule of EA to form a di-addition product (selectivity < 3%).

Intermolecular hydroamination of EA with aniline was carried out using AlSBA-15 with different Si/Al and results are presented in Table 1. It is seen that AlSBA-15 (10) showed highest activity with 77% EA conversion and the others followed as AlSBA-15 (20) (60%), AlSBA-15 (30) (41%) and AlSBA-15 (40) (33%) after 6 h of reaction. The results indicate that the conversion increases with decrease in Si/Al ratios, i.e. increase in acidity. AlMCM-41 (Si/Al = 15) gave slightly more conversion compared to AlSBA-15 (10) (Si/Al = 17) but lower TOF (43) (expressed as moles of EA converted per mole Al per hour). The activities of well known heterogeneous catalysts such as H-beta and montmorillonite K-10 were compared with mesoporous solid acids. Interestingly highly acidic H-beta was only half as active as AlSBA-15 (conversion = 41% and TOF = 18). Lower activity of H-beta can be attributed to its smaller pore size which restricts the mobility of the molecules. Previous reports on Zn-beta and CuAlSBA-15 catalysts showed that Lewis acidic Cu^{2+} and Zn^{2+} catalyze hydroamination of alkynes by aromatic amines [40,45]. Hence, the activities of ZnAlSBA-15 and CuAlSBA-15 catalysts were compared with AlSBA-15 catalysts. Interestingly, there is a decrease in EA conversion after Cu and Zn exchange with AlSBA-15. The result

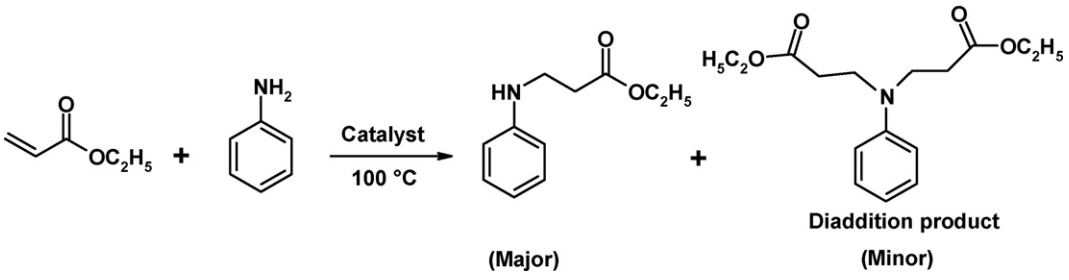

Scheme 1.

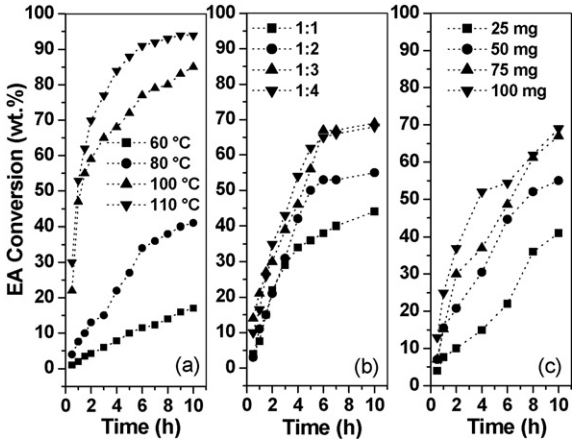

Fig. 6. Effect of reaction conditions: (a) effect of reaction temperature, conditions: catalyst = AlSBA-15 (10), aniline to EA mole ratio = 1, catalyst wt. = 0.05 g, total reactants wt. = 2 g, toluene = 3 ml; (b) effect of aniline to EA mole ratio, conditions: catalyst = AlSBA-15 (10), temperature = 80° C, catalyst wt. = 0.05 g, total reactants wt. = 2 g, toluene = 3 ml; (c) effect of catalyst concentration, conditions: catalyst = AlSBA-15 (10), temperature = 80° C, aniline to EA mole ratio = 1, total reactants wt. = 2 g, toluene = 3 ml.

clearly shows that the Brönsted acidity in AlSBA-15 catalyzes the hydroamination of activated olefins.

Hydroamination of EA with aniline reaction was studied by varying the temperatures (60–110 °C), keeping constant catalyst 0.05 g (2% of the total reactant weight) and aniline to EA mole ratio as 1. Conversion of EA as a function of time is shown in Fig. 6(a). The anti-Markovnikov addition product *N*-[2-(ethoxycarbonyl)ethyl]aniline formed with 100% selectivity. The results show that the activity (conversion of EA) of the catalyst increases substantially with increasing reaction temperature. At 60 °C, the conversion was only 17%, which increased to 94% at 110 °C in 10 h of reaction. Following the initial rate approach, the graph of ln(rate) versus 1/*T* was plotted, which gave a straight line and the activation energy calculated from the slope was found to be 20 kcal/mol.

The reaction was also carried out with aniline to EA molar ratios ranging from 1 to 4 keeping catalyst wt. (0.05 g) and temperature (80 °C) constant and the results are shown in Fig. 6(b). The results show that the conversion of EA increased from 36 to 62% on varying the molar ratio from 1 to 4 over a period of 5 h. However, the change in the mole ratio did not affect the selectivity. The anti-Markovnikov addition product formed with 100% selectivity. But excess of EA in the reaction decreases the selectivity of mono-addition product because it reacts further with another molecule of EA to form di-addition product.

The effect of catalyst concentration on EA conversion was studied at 80 °C with aniline/EA mole ratio of 1 (Fig. 6(c)). It shows that as the catalyst concentration increased, the conversion of EA increased as expected. There was linear increase in conversion up to 8 h and the reaction is slowed down with marginal increase in the range of 8–10 h. At optimized reaction conditions; 100 °C, aniline to EA molar ratio of 2, catalyst weight 0.1 g and total reactant weight 2 g and 3 ml of toluene as a solvent, the conversion of EA was found to be 99% with 98% selectivity for mono-addition product after 15 h reaction.

In order to check the leaching of framework Al into the reaction mixture during the course of the reaction, reaction was carried out for 2 h under selected reaction conditions. The reaction was then stopped and catalyst was separated by filtration of hot reaction mixture and same reaction mixture was stirred further for 10 h. It was found that in the absence of the catalyst, there was no further increase in the conversion of EA, which indicated the absence of leaching of Al. The above study ensured that the reaction was catalyzed purely by a heterogeneous catalyst.

Table 2
Hydroamination of different activated olefins and amines catalyzed by AlSBA-15 (10)

Aromatic amine	Activated olefin	Time (h)	Yield (%)	Anti-Markovnikov product selectivity (%)	
				Mono-addition	Di-addition
Aniline	Ethyl acrylate	4	75	99	1
		10	93	98	2
4-Bromoaniline	Ethyl acrylate	4	40	100	0
		10	68	98	2
p-Anisidine	Ethyl acrylate	4	65	99	1
		10	91	97	3
2,4-Xylidene	Ethyl acrylate	4	59	99	1
		10	85	98	2
o-Nitroaniline	Ethyl acrylate	20	NR	–	–
p-Ethylaniline	Ethyl acrylate	4	82	100	0
		10	95	99	1
N-Methylaniline	Ethyl acrylate	4	50	100	0
		10	71	99	1
1-Naphthylamine	Ethyl acrylate	4	40	100	0
		10	65	100	0
Cyclohexylamine	Ethyl acrylate	2	95	100	0
Aniline	Methyl acrylate	10	65	100	0
Aniline	Acrylonitrile	10	21	100	0
Aniline	Acrylic acid	10	40	100	0

Reaction conditions: temperature = 100 °C, amine: activated olefin = 1 (molar ratio), catalyst wt. = 0.1 g, total reactants wt. = 2 g, yield of mono-addition product was determined by GC analysis, NR = No reaction.

The recyclability of AlSBA-15 (10) catalyst was tested in the hydroamination of EA with aniline by conducting five runs (~85% conversion after 10 h) using selected reaction conditions. After each run, the catalyst was repeatedly washed with toluene, dried at 120 °C for 2 h and calcined at 500 °C in air for 2 h. It was then used in the hydroamination reaction with a fresh reaction mixture. It was found that the conversion was practically the same in all the five cycles.

To further investigate the reaction, we carried out the reaction of aniline with different α, β-ethylenic compounds like methyl acrylate, acrylonitrile and acrylic acid with 5 wt% AlSBA-15 (10), at 100 °C and molar ratio of 1 (Table 2). The yield for mono-addition product was obtained in the order EA (93%) > methyl acrylate (65%) > acrylic acid (40%) > acrylo nitrile (18%) after 10 h of reaction. Since aniline is basic, it undergoes a side reaction with acrylic acid to form acrylanilide.

To explore the general applicability of the catalyst, hydroaminations of EA with different amines were carried out and the mono-addition product yield after 10 h of reaction was compared (Table 2). The nature of substituents on the aromatic ring of aniline derivatives has considerable effect over the reactivity. The electron-donating groups at the *-ortho* and *-para* positions gave higher yields of mono-addition, anti-Markovnikov products. Large molecule such as 1-naphthylamine gave a higher yield (65%), which indicates that the bulky amines can easily pass through the mesopores of AlSBA-15. The aromatic amines with electron withdrawing substituents such as 4-bromoaniline (21%) were less reactive, whereas *p*-nitroaniline did not undergo reaction with EA. The results showed that AlSBA-15 can also be used for hydroamination using secondary amine (*N*-methylaniline, 71% yield) and aliphatic amines (cyclohexylamine, 95% yield). These results indicate that the amine reactivity depends on their basicity. It is well known that aliphatic amines are more basic than aromatic amines, whereas amines with electron donating substituents are more basic than amines with electron withdrawing substituents. As the basicity of amines increased their reactivity also increased in hydroamination of activated olefins and *vice versa*.

4. Conclusions

β-Amino acid derivatives were synthesized by hydroamination reaction of activated olefins with amines using AlSBA-15 catalyst. AlSBA-15 was synthesized by isomorphous substitution of aluminium into SBA-15 framework, which induces the Brönsted and Lewis acid sites. The catalytic activities of AlSBA-15 and AlMCM-41 were found to be approximately double compared to H-beta and montmorillonite K-10. Hydroamination of ethyl acrylate (EA) with aniline has been used as a test reaction, which gave anti-Markovnikov product *N*-[2-(ethoxycarbonyl)ethyl]aniline with high selectivity. The activities of the catalysts depended on the total acidity and as well as both Brönsted and Lewis acid sites, which are active centers for hydroamination reaction. The catalyst showed higher activities for hydroamination of EA with aliphatic amines, secondary amines and aromatic amines with electron donating substituents.

Acknowledgement

G.V.S acknowledges CSIR, New Delhi for awarding Senior Research Fellowship.

References

[1] T.E. Müller, M. Beller, Chem. Rev. 98 (1998) 675.
[2] J.J. Brunet, D. Neibecker, in: A. Togni, H. Grützmacher (Eds.), Catalytic Heterofunctionalization, Wiley–VCH, Weinheim, 2001, pp. 91–141.
[3] F. Pohlki, S. Doye, Chem. Soc. Rev. 32 (2003) 104.
[4] L.L. Anderson, J. Arnold, R.G. Bergman, J. Am. Chem. Soc. 127 (2005) 14543.
[5] J.A. Bexrud, J.D. Beard, D.C. Leitch, L.L. Schafer, Org. Lett. 7 (2005) 1959.
[6] L. Ackermann, L.T. Kaspar, A. Althammer, Org. Biomol. Chem. 5 (2007) 1975 (and references cited there in).
[7] O. Jimenez, T.E. Müller, C. Sievers, A. Spirkl, J.A. Lercher, Chem. Commun. (2006) 2974.
[8] N. Sewald, Amino Acids 11 (1996) 397.
[9] E. Juaristi, H.L. Ruiz, Curr. Med. Chem. 6 (1999) 983.
[10] M. Perez, R. Pleixats, Tetrahedron 51 (1995) 8355.
[11] T.C. Wabnitz, J.B. Spencer, Org. Lett. 5 (2003) 2141.
[12] L.W. Xu, J.W. Li, C.G. Xia, S.L. Zhou, X.X. Hu, Syn. Lett. 15 (2003) 2425.
[13] J. Monfray, A.M.P. Koskinen, Lett. Org. Chem. 3 (2006) 324.
[14] J.J. Bozell, L.S. Hegedus, J. Org. Chem. 46 (1981) 2561.
[15] L. Fadini, A. Togni, Chem. Commun. (2003) 30.
[16] N.S. Shaikh, V.H. Deshpande, A.V. Bedekar, Tetrahedron 57 (2001) 9045.
[17] J. Horniakova, K. Komura, H. Osaki, Y. Kubota, Y. Sugi, Catal. Lett. 102 (2005) 191.
[18] M.L. Kantam, B. Nilima, C.V. Reddy, J. Mol. Catal. A Chem. 241 (2005) 147.
[19] T. Joseph, G.V. Shanbhag, D.P. Sawant, S.B. Halligudi, J. Mol. Catal. A Chem. 250 (2006) 210.
[20] M. Tada, M. Shimamoto, T. Sasaki, Y. Iwasawa, Chem. Commun. (2004) 2562.
[21] S. Lin, L.F. Wang, Y. Han, Y. Yu, Y. Di, R.W. Wang, D.Z. Jiang, F.S. Xiao, Chin. J. Chem. 22 (2004) 9.
[22] R. Ryoo, S. Jun, J.M. Kim, M.J. Kim, Chem. Commun. (1997) 2225.
[23] Y. Yue, A. Cedeon, J.L. Bonardet, N. Melosh, J.B. Despinose, J. Fraissard, Chem. Commun. (1999) 1967.
[24] A. Vinu, V. Murugesan, W. Böhlmann, M. Hartmann, J. Phys. Chem. B 108 (2004) 11496.
[25] A. Vinu, B.M. Devassy, S.B. Halligudi, W. Böhlmann, M. Hartmann, Appl. Catal. A: Gen. 281 (2005) 207.
[26] A. Vinu, G.S. Kumar, K. Ariga, V. Murugesan, J. Mol. Catal. A: Chem. 235 (2005) 57.
[27] W. Li, S.J. Huang, S.B. Liu, M.O. Coppens, Langmuir 21 (2005) 2078.
[28] Y. Li, Q. Yang, J. Yang, C. Li, J. Porous Mater. 13 (2006) 187.
[29] M. Xu, W. Wang, M. Seiler, A. Buchholz, M. Hunger, J. Phys. Chem. B 106 (2002) 3202.
[30] M.A. Zanjanchi, S. Asgari, Solid State Ionics 171 (2004) 277.
[31] R. Luque, J.M. Campelo, D. Luna, J.M. Marinas, A.A. Romero, Micropor. Mesopor. Mater. 84 (2005) 11.
[32] Z. Luan, M. Hartmann, D. Zhao, W. Zhou, L. Kevan, Chem. Mater. 11 (1999) 1621.
[33] M. Cheng, Z. Wang, K. Sakurai, F. Kumata, T. Saito, T. Komatsu, T. Yashima, Chem. Lett. 2 (1999) 131.
[34] S. Sumiya, Y. Oumi, T. Uozumi, T. Sano, J. Mater. Chem. 11 (2001) 1111.
[35] H.M. Kao, C.C. Ting, S.W. Chao, J. Mol. Catal. A: Chem. 235 (2005) 200.
[36] M.G. Cazalilla, J.M.M. Robles, A. Gurbani, E.R. Castellon, A.J. Lopez, J. Solid State Chem. 180 (2007) 1130.
[37] G.V. Shanbhag, S.B. Halligudi, J. Mol. Catal. A Chem. 222 (2004) 223.
[38] T. Joseph, G.V. Shanbhag, S.B. Halligudi, J. Mol. Catal. A Chem. 236 (2005) 139.

[39] G.V. Shanbhag, S.M. Kumbar, T. Joseph, S.B. Halligudi, Tetrahedron Lett. 47 (2006) 141.
[40] G.V. Shanbhag, T. Joseph, S.B. Halligudi, J. Catal. 250 (2007) 274.
[41] D. Zhao, J. Feng, Q. Huo, N. Melosh, G.H. Fredrickson, B.F. Chmelka, G.D. Stucky, Science 279 (1998) 548.
[42] A. Bordoloi, B.M. Devassy, P.S. Niphadkar, P.N. Joshi, S.B. Halligudi, J. Mol. Catal. A 253 (2006) 239.
[43] W. Kolodziejski, A. Corma, M.T. Navarro, J. Perez-Periente, Solid State Nucl. Magn. Reson. 2 (1993) 253.
[44] R. Anwander, C. Palm, G. Gerstberger, O. Groeger, G. Engelhardt, Chem. Commun. (1998) 1811.
[45] J. Penzien, T.E. Muller, J.A. Lercher, Micropor. Mesopor. Mater. 48 (2001) 285.